Journal of
Mechanics of Materials and Structures

VIBRATION CHARACTERISTICS OF CURVED BEAMS

Chong-Seok Chang and Dewey H. Hodges

Volume 4, Nº 4 *April 2009*

mathematical sciences publishers

JOURNAL OF MECHANICS OF MATERIALS AND STRUCTURES
Vol. 4, No. 4, 2009

VIBRATION CHARACTERISTICS OF CURVED BEAMS

CHONG-SEOK CHANG AND DEWEY H. HODGES

The paper presents a concise framework studying the coupled vibration of curved beams, whether the curvature is built-in or is caused by loading. The governing equations used are both geometrically exact and fully intrinsic, with a maximum degree of nonlinearity equal to two. For beams with initial curvature, the equations of motion are linearized about the reference state. For beams that are curved because of the loading, the equations of motion are linearized about the equilibrium state. A central difference spatial discretization scheme is applied, and the resulting linearized ordinary differential equations are cast as an eigenvalue problem. Numerical examples are presented, including: (1) validation of the analysis for both in-plane and out-of-plane vibration by comparison with published results, and (2) presentation of results for vibration of curved beams with free-free, clamped-clamped, and pinned-pinned boundary conditions. For coupled vibration, the numerical results also exhibit the low-frequency mode transition or veering phenomenon. Substantial differences are also shown between the natural frequencies of curved beams and straight beams, and between initially curved and bent beams with the same geometry.

1. Introduction

For decades, the vibration of curved beams, rings, and arches has been extensively investigated by many researchers. About 400 references, which have covered the in-plane (i.e. in the plane of the undeformed, initially curved beam), out-of-plane (i.e. out of the plane of the undeformed, initially curved beam), coupled, and nonlinear vibrations, are summarized in [Chidamparam and Leissa 1993]. While linear theory is adequate for free-vibration analysis of initially curved beams, when a beam is brought into a state of high curvature by the loads acting on it, one must linearize the equations of nonlinear theory about the static equilibrium state. Thus, the behavior of a beam curved under load will differ substantially from an initially curved beam of identical geometry. The geometrically exact, fully intrinsic theory of curved and twisted beams [Hodges 2003] provides an excellent framework in which to elegantly study the coupled vibration characteristics of curved beams, particularly those curved because they are loaded. This is because of their simplicity. Each term can be intuitively interpreted. There are no displacement or rotation variables (which is what is meant by intrinsic in this context); as a result there are no nonlinearities of degree larger than two. Both finite element and finite difference discretization schemes are easily applied to these equations for numerical computations, and the framework presented herein is much simpler than that of other nonlinear beam theories. Because of these observations, we have revisited the topic and broadened the base of cases studied.

This paper provides details of how to make use of the fully intrinsic equations for calculating natural frequencies for simple engineering problems. One aspect of these calculations that is substantially different from the usual approach involves the proper way to enforce boundary conditions. Published results

Keywords: vibration, curved beams, nonlinear, intrinsic.

for in-plane [Chidamparam and Leissa 1995; Tarnopolskaya et al. 1996; Fung 2004] and out-of-plane vibration [Irie et al. 1982; Howson and Jemah 1999] will be compared with the results from the present work. Results for coupled vibration are also presented as part of an investigation of low-frequency mode transition [Tarnopolskaya et al. 1999], also referred to as veering phenomena [Chen and Ginsberg 1992].

It was shown analytically in [Hodges 1999] that initially curved, isotropic beams possess stretch-bending elastic coupling, that this coupling is proportional to initial curvature when the beam reference line is along the locus of cross-sectional centroids, and that this coupling cannot be ignored for calculation of the equilibrium state of high circular arches. The Variational Asymptotic Beam Sectional (VABS) analysis [Cesnik and Hodges 1997; Yu et al. 2002; Hodges 2006] can be used to numerically calculate this coupling term. Based on results obtained from VABS, it is easy to show that there is another term, which also depends on initial curvature but reflects shear-torsion coupling. This term becomes zero if the beam reference axis is along the locus of sectional shear centers rather than the locus of sectional centroids. The location of the sectional shear center depends on the initial curvature, but an analytical expression for that dependence is unknown. Therefore, without a cross-sectional analysis tool such as VABS, which provides an accurate cross-sectional stiffness matrix as a function of initial curvature, certain aspects of the analysis presented herein would be impossible.

2. Intrinsic beam formulation

The geometrically exact, intrinsic governing equations [Hodges 2003] for the dynamics of an initially curved and twisted, generally anisotropic beam are

$$\begin{aligned} F_B' + \widetilde{K}_B F_B + f_B &= \dot{P}_B + \widetilde{\Omega}_B P_B, \\ M_B' + \widetilde{K}_B M_B + (\tilde{e}_1 + \tilde{\gamma}) F_B + m_B &= \dot{H}_B + \widetilde{\Omega}_B H_B + \widetilde{V}_B P_B, \\ V_B' + \widetilde{K}_B V_B + (\tilde{e}_1 + \tilde{\gamma}) \Omega_B &= \dot{\gamma}, \\ \Omega_B' + \widetilde{K}_B \Omega_B &= \dot{\kappa}, \end{aligned} \tag{1}$$

where F_B and M_B are the internal force and moment measures, P_B and H_B are the sectional linear and angular momenta, V_B and Ω_B are the velocity and angular velocity measures, γ and κ are the force and moment strain measures, k contains the initial twist and curvature measures of the beam, $K_B = k + \kappa$ contains the total curvature measures, and f_B and m_B are external force and moment measures, where loads such as gravitational, aerodynamic, and mechanical applied loads are taken into account. All quantities are expressed in the basis of the deformed beam cross-sectional frame except k which is in the basis of the undeformed beam cross-sectional frame. The tilde operator as in $\tilde{a}b$ reflects a matrix form of the cross product of vectors $\mathbf{a} \times \mathbf{b}$ when both vectors and their cross product are all expressed in a common basis.

A central difference discretization scheme is applied to the intrinsic governing equations in space to obtain a numerical solution. The scheme satisfies both of the space-time conservation laws derived in [Hodges 2003]. This scheme can be viewed as equivalent to a particular finite element discretization, and the intrinsic governing equations are expressed as element and nodal equations. The n-th element

equations, which are a spatially discretized form of (1), are

$$\begin{aligned}
\frac{\widehat{F}_l^{n+1}-\widehat{F}_r^n}{dl}+(\widetilde{\overline{\kappa}}^n+\widetilde{\overline{k}}^n)\overline{F}^n+\overline{f}^n-\dot{\overline{P}}^n-\widetilde{\overline{\Omega}}^n\overline{P}^n=0,\\
\frac{\widehat{M}_l^{n+1}-\widehat{M}_r^n}{dl}+(\widetilde{\overline{\kappa}}^n+\widetilde{\overline{k}}^n)\overline{M}^n+(\widetilde{e}_1+\widetilde{\overline{\gamma}}^n)\overline{F}^n+\overline{m}^n-\dot{\overline{H}}^n-\widetilde{\overline{\Omega}}^n\overline{H}^n-\widetilde{\overline{V}}^n\overline{P}^n=0,\\
\frac{\widehat{V}_l^{n+1}-\widehat{V}_r^n}{dl}+(\widetilde{\overline{\kappa}}^n+\widetilde{\overline{k}}^n)\overline{V}^n+(\widetilde{e}_1+\widetilde{\overline{\gamma}}^n)\overline{\Omega}^n-\dot{\overline{\gamma}}^n=0,\\
\frac{\widehat{\Omega}_l^{n+1}-\widehat{\Omega}_r^n}{dl}+(\widetilde{\overline{\kappa}}^n+\widetilde{\overline{k}}^n)\overline{\Omega}^n-\dot{\overline{\kappa}}^n=0,
\end{aligned}\tag{2}$$

where dl is the element length. The variables with $\widehat{(\,)}$ are nodal variables, and the superscript indicates the corresponding node where the variable is defined. Nodal variables are defined at both the left and right of nodes, which are indicated by subscript l and r. The variables with $\overline{(\,)}$ are element variables. (The details of discretization are described in [Hodges 2003].)

The equations for node n need to include possible discontinuities caused by a nodal mass, a nodal force, and slope discontinuity, so that

$$\begin{aligned}
\widehat{F}_r^n-\widehat{C}_{lr}^{n^T}\widehat{F}_l^n+\widehat{f}^n-\dot{\widehat{P}}_r^n-\widetilde{\widehat{\Omega}}_r^n\widehat{P}_r^n=0,\\
\widehat{M}_r^n-\widehat{C}_{lr}^{n^T}\widehat{M}_l^n+\widehat{m}^n-\dot{\widehat{H}}_r^n-\widetilde{\widehat{\Omega}}_r^n\widehat{H}_r^n-\widetilde{\widehat{V}}_r^n\widehat{P}_r^n=0,
\end{aligned}\tag{3}$$

where $\widehat{C}_{lr}$ reflects the slope discontinuity, $\widehat{f}^n$ and $\widehat{m}^n$ are external forces and moments applied at n-th node, and

$$\widehat{V}_l^n=\widehat{C}_{lr}^n\widehat{V}_r^n,\qquad \widehat{\Omega}_l^n=\widehat{C}_{lr}^n\widehat{\Omega}_r^n.\tag{4}$$

One may also include gravitational force in the analysis. When this is done, the formulation needs additional gravity equations, details of which may be found in [Patil and Hodges 2006].

3. Boundary conditions

Boundary conditions are needed to complete the formulation. Here, we describe boundary conditions for simple engineering problems, such as pinned-pinned and clamped-clamped conditions. At each end, for the static case, either natural boundary conditions in terms of $\widehat{F}$ and $\widehat{M}$ or geometric boundary conditions in terms of u and C^{iB} may be prescribed. Here u is a column matrix of displacement measures u_i in the cross-sectional frame of the undeformed beam. Although these geometric boundary conditions are in terms of displacement and rotation variables, they are easily expressed in terms of other variables such as κ, γ, etc., given in (13), keeping the formulation intrinsic.

If displacement and rotation variables appear in the boundary conditions for the free-vibration case, a numerical Jacobian would become necessary since determination of an analytical expression for it is intractable. Fortunately, when calculating free-vibration frequencies, one may for convenience replace boundary conditions on displacement and rotation variables with boundary conditions in terms of generalized velocities $\widehat{V}$ and $\widehat{\Omega}$. With the use of velocity boundary conditions, however, rigid-body modes will not be eliminated from the results.

3.1. ***Pinned-pinned boundary conditions.*** A total of 12 boundary conditions is necessary to calculate free-vibration frequencies, given by

$$\widehat{V}_l^1 = \widehat{M}_l^1 = 0, \tag{5}$$

$$\widehat{V}_r^{N+1} = 0 \quad \text{or} \quad \begin{cases} e_1^T C^{iB^{N+1}} \widehat{F}_r^{N+1} = 0, \\ e_2^T \widehat{V}_r^{N+1} = 0, \\ e_3^T C^{iB^{N+1}} \widehat{V}_r^{N+1} = 0, \end{cases} \tag{6}$$

$$\widehat{M}_r^{N+1} = 0, \tag{7}$$

where $C^{iB^{N+1}}$ is the rotation matrix of the beam cross-section at the right end. Equation (5) fixes the left boundary in space but leaves it free to rotate about all three axes. One can apply a geometric boundary condition of zero displacement at the left end. One may take advantage of the intrinsic formulation through applying the velocity boundary condition given in (5). The right boundary condition of (6) allows free movement in the axial direction while holding velocity components in the transverse directions to zero, as shown in the right part of Figure 1. When there are no applied loads, one can simply make use of trivial values as the state about which the equations are linearized.

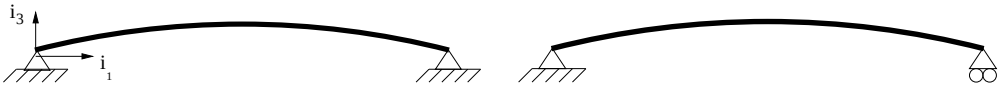

Figure 1. Schematics of initially curved beams with pinned-pinned boundary conditions.

For a loaded case, however, the state about which the equations are linearized should be the static equilibrium state. To determine the static equilibrium, six boundary conditions are necessary. (For static equilibrium, the equations for V and Ω, namely $(2)_3$ and $(2)_4$, become trivial. That reduces the number of boundary conditions to 6 from 12.) They are given by $\widehat{M}_l^1 = 0$ and

$$\begin{gathered} u_1^{N+1} = 0 \quad \text{or} \quad e_1^T C^{iB^{N+1}} \widehat{F}_r^{N+1} = 0, \\ u_2^{N+1} = u_3^{N+1} = 0. \end{gathered} \tag{8}$$

The right end can be chosen either free to move in the axial direction or to be fixed in space, which is described in (8). For static equilibrium, one must apply displacement boundary conditions, which appear in (8).

3.2. ***Clamped-clamped boundary conditions.*** The boundary conditions are

$$\widehat{V}_l^1 = \widehat{\Omega}_l^1 = 0 \tag{9}$$

Figure 2. Initially curved beam with clamped-clamped boundary condition.

and

$$\widehat{V}_r^{N+1} = \widehat{\Omega}_r^{N+1} = 0 \tag{10}$$

Equations (9) and (10) are for boundaries that are fixed in space and which constrain the rotation about all three axes to be zero.

Like the pinned-pinned boundary condition, for a loaded case, the boundary conditions for a static equilibrium are

$$u_{\text{def}}^{N+1} = 0, \tag{11}$$

$$\widehat{C}_{\text{undef}}^{iB^{N+1}{}^T} \widehat{C}_{\text{def}}^{iB^{N+1}} = \Delta, \tag{12}$$

where u_{def} is the column matrix of displacement measures at the right end of the beam, and $\widehat{C}_{\text{def}}^{iB^{N+1}}$, $\widehat{C}_{\text{undef}}^{iB^{N+1}}$ are the rotation matrices of the beam cross-section at the right end after deformation and in the undeformed state, respectively.

The geometric boundary conditions for static equilibrium can be described by the generalized strain-displacement equations from [Hodges 2003], namely

$$(r+u)' = C^{iB}(\gamma + e_1), \qquad C^{Bi\,\prime} = -(\widetilde{\kappa} + \widetilde{k})C^{Bi}, \tag{13}$$

where r is the column matrix of position vector measures and u is the column matrix of displacement measures, both in the undeformed beam cross-sectional basis, and C^{Bi} is the rotation matrix of the beam cross-sectional reference frame in the deformed configuration. Equations (13) can be discretized as

$$\begin{aligned} r^{n+1} + u^{n+1} &= r^n + u^n + \overline{C}^{iB^n}(\overline{\gamma}^n + e_1)dl \\ \widehat{C}^{Bi^{n+1}} &= \left(\frac{\Delta}{dl} + \frac{\widetilde{\overline{\kappa}} + \widetilde{k}^n}{2}\right)^{-1} \left(\frac{\Delta}{dl} - \frac{\widetilde{\overline{\kappa}} + \widetilde{k}^n}{2}\right) \widehat{C}^{Bi^n} \end{aligned} \tag{14}$$

4. Linearization

The governing equations in the previous section are linearized about a static equilibrium so that they reduce to an eigenvalue problem to calculate the vibration frequencies. First,

$$X = X_{\text{eq}} + X^*(t) \tag{15}$$

where X is a state, X_{eq} is a value of the state at a static equilibrium, and X^* is a small perturbation about the static value of the state. The linearized element equations from the intrinsic beam formulation are then

$$\begin{aligned} \frac{\widehat{F}_l^{*n+1} - \widehat{F}_r^{*n}}{dl} + (\widetilde{\overline{\kappa}}_{\text{eq}}^n + \widetilde{k}^n)\overline{F}^{*n} + \widetilde{\overline{\kappa}}^{*n}\overline{F}_{\text{eq}}^n + \mu^n \bar{g}^{*n} &= \dot{\bar{P}}^{*n}, \\ \frac{\widehat{M}_l^{*n+1} - \widehat{M}_r^{*n}}{dl} + (\widetilde{\overline{\kappa}}_{\text{eq}}^n + \widetilde{k}^n)\overline{M}^{*n} + \widetilde{\overline{\kappa}}^{*n}\overline{M}_{\text{eq}}^n + (\widetilde{e}_1 + \widetilde{\overline{\gamma}}_{\text{eq}}^n)\overline{F}^{*n} + \widetilde{\overline{\gamma}}^{*n}\overline{F}_{\text{eq}}^n + \mu^n \widetilde{\xi}^n \bar{g}^{*n} &= \dot{\bar{H}}^{*n}, \\ \frac{\widehat{V}_l^{*n+1} - \widehat{V}_r^{*n}}{dl} + (\widetilde{\overline{\kappa}}_{\text{eq}}^n + \widetilde{k}^n)\overline{V}^{*n} + (\widetilde{e}_1 + \widetilde{\overline{\gamma}}_{\text{eq}}^n)\overline{\Omega}^{*n} &= \dot{\bar{\gamma}}^{*n}, \\ \frac{\widehat{\Omega}_l^{*n+1} - \widehat{\Omega}_r^{*n}}{dl} + (\widetilde{\overline{\kappa}}_{\text{eq}}^n + \widetilde{k}^n)\overline{\Omega}^{*n} &= \dot{\bar{\kappa}}^{*n}. \end{aligned} \tag{16}$$

The linearized nodal equations are

$$\widehat{F}_r^{*n} - \widehat{C}_{lr}^{n^T}\widehat{F}_l^{*n} + \widehat{\mu}^n\widehat{g}_r^{*n} - \dot{\widehat{P}}_r^{*n} = 0, \qquad \widehat{M}_r^{*n} - \widehat{C}_{lr}^{n^T}\widehat{M}_l^{*n} + \widehat{\mu}^n\widetilde{\widehat{\xi}}^n\widehat{g}_r^{*n} - \dot{\widehat{H}}_r^{*n} = 0. \tag{17}$$

These linearized equations of motion can be expressed in matrix form as $A\dot{\widehat{X}} = B\widehat{X}$, which is a system of first-order equations. When $\widehat{X} = \check{X}\exp(\lambda t)$ is assumed, the system is easily cast as a generalized eigenvalue problem of the form

$$B\check{X} = A\lambda\check{X}. \tag{18}$$

When B^{-1} exists, the equation can be rearranged into a standard eigenvalue problem, such that

$$\frac{1}{\lambda}\check{X} = B^{-1}A\check{X}, \qquad A^*\check{X} = \lambda^*\check{X}. \tag{19}$$

When the eigenvalues are pure imaginary, the motion is of simple harmonic type.

5. Validation

A typical cross-sectional model has the form

$$\begin{Bmatrix} \gamma_{11} \\ 2\gamma_{12} \\ 2\gamma_{13} \\ \kappa_1 \\ \kappa_2 \\ \kappa_3 \end{Bmatrix} = \begin{bmatrix} R_{11} & R_{12} & R_{13} & S_{11} & S_{12} & S_{13} \\ R_{12} & R_{22} & R_{23} & S_{21} & S_{22} & S_{23} \\ R_{13} & R_{23} & R_{33} & S_{31} & S_{32} & S_{33} \\ S_{11} & S_{21} & S_{31} & T_{11} & T_{12} & T_{13} \\ S_{12} & S_{22} & S_{32} & T_{12} & T_{22} & T_{23} \\ S_{13} & S_{23} & S_{33} & T_{13} & T_{23} & T_{33} \end{bmatrix} \begin{Bmatrix} F_1 \\ F_2 \\ F_3 \\ M_1 \\ M_2 \\ M_3 \end{Bmatrix}, \qquad \begin{Bmatrix} \gamma \\ \kappa \end{Bmatrix} = \begin{bmatrix} R_{3\times3} & S_{3\times3} \\ S_{3\times3}^T & T_{3\times3} \end{bmatrix} \begin{Bmatrix} F \\ M \end{Bmatrix}, \tag{20}$$

where the 3×3 submatrices R, S, and T, which make up the cross-sectional flexibility matrix, are computed by VABS [Cesnik and Hodges 1997; Yu et al. 2002; Hodges 2006] for various initial curvatures. Though not essential, to make the shear-torsion elastic couplings $S_{21} = S_{31} = 0$, the stiffness matrix may be recomputed at the cross-sectional shear center.

In-plane and out-of-plane vibrations are separately validated by comparison with results from various published papers. Either in-plane or out-of-plane vibration can be approximated by setting some of the components in the submatrices equal to very small values, which minimally affects the results. For example, for inextensibility, one would simply set R_{11} to a very small value; for shear indeformability one would set R_{22} and R_{33} to very small values. Likewise, one could set certain elements of the flexibility matrix equal to very small values to approximate either in-plane or out-of-plane vibrations. Setting these small numbers equal to zero may result in the problem's becoming ill-conditioned because, for certain boundary conditions, a variable cannot be assumed to be zero unless the associated governing equations and variables are eliminated from the formulation. For the same reason, one should not set certain components too small for a given boundary condition.

Example: in-plane free-vibration of curved beams with different half-angles. The beam investigated has length $\ell = 10$ m and an initial curvature such that $hk_2 = h/R_r = 0.01$ where ℓ is the total length of beam, h is the thickness of the cross-section, $R_r = 1/k_2$ is the radius of the curved beam (or arch), and α is the half-angle of the arch ($\ell = 2R_r\alpha$). For beams of constant length, α is clearly a measure of the initial curvature. Values associated with $\alpha = 10^\circ$ and 30° are selectively given in Table 1. For $h/R_r = 0.01$ and

$\ell = 10$ m, the nondimensional frequencies of an arch having a rectangular cross-section are calculated for both pinned-pinned and clamped-clamped boundary conditions. Results obtained are given in Tables 2 and 3. For the pinned-pinned boundary, both ends are fixed in space but free to rotate about an axis perpendicular to the plane of the undeformed beam, which is the left case of Figure 1. The results agree well with those of [Chidamparam and Leissa 1995] for both extensible and inextensible cases.

	Example 1: in-plane			
	extensible		inextensible	
α	10°	30°	10°	30°
R_{11}	1.7407e-10	1.5667e-09	1.7407e-15	1.5667e-14
R_{22}	5.7624e-15	5.1862e-14	5.7624e-15	5.1862e-14
R_{33}	5.7623e-15	5.1861e-14	5.7623e-15	5.1861e-14
S_{12}	1.4477e-11	3.9088e-10	1.4477e-16	3.9088e-15
S_{21}	1.7517e-19	4.6425e-18	1.7517e-19	4.6425e-18
T_{11}	4.1277e-13	3.3435e-11	4.1277e-13	3.3435e-11
T_{22}	2.5451e-08	2.0616e-06	2.5451e-08	2.0616e-06
T_{33}	2.5451e-13	2.0616e-11	2.5451e-13	2.0616e-11
R_r	28.648	9.5493	28.648	9.5493
$h = b$	2.8648e-01	9.5493e-02	2.8648e-01	9.5493e-02
ξ_3	2.5092e-04	8.3638e-05	2.5092e-04	8.3638e-05

	Example 2: out-of-plane					
	$\sigma_2 = \sigma_3 = 20$			$\sigma_2 = \sigma_3 = 100$		
α	30°	60°	90°	30°	60°	90°
R_{11}	2.1039e-11	8.4156e-11	1.8935e-10	5.2235e-10	2.0894e-09	4.7012e-09
R_{22}	6.9672e-11	2.7869e-10	6.2705e-10	1.7292e-09	6.9166e-09	1.5563e-08
R_{33}	6.9327e-16	2.7731e-15	6.2394e-15	1.7289e-14	6.9153e-14	1.5560e-13
S_{12}	1.0467e-16	8.3736e-16	2.8260e-15	2.6082e-15	2.0864e-14	7.0451e-14
S_{21}	3.9071e-14	3.1195e-13	1.0694e-12	3.6632e-14	3.2723e-13	−4.2443e-12
T_{11}	5.8829e-10	9.4127e-09	4.7652e-08	3.7136e-07	5.9415e-06	3.0081e-05
T_{22}	3.6587e-15	5.8539e-14	2.9635e-13	2.2905e-12	3.6646e-11	1.8553e-10
T_{33}	3.6465e-10	5.8344e-09	2.9537e-08	2.2902e-07	3.6642e-06	1.8551e-05
R_r	4.7746	2.3873	1.5915	4.7746	2.3873	1.5915
$h = b$	8.2699e-01	4.1349e-01	2.7566e-01	1.6539e-01	8.2699e-02	5.5133e-02
ξ_3	1.2655e-02	6.3274e-03	4.2183e-03	5.0199e-04	2.5100e-04	1.6733e-04

Table 1. Nonzero cross-sectional constants used for validation of in-plane and out-of plane free-vibration results (flexibility submatrices R_{ij}, S_{ij}, T_{ij}, radius of curvature R_r, thickness of cross-section h, width of cross-section b, shear center location ξ_3)

	extensible case							
	[Chidamparam and Leissa 1995]				Current approach			
α	mode 1	mode 2	mode 3	mode 4	mode 1	mode 2	mode 3	mode 4
5°	449.38	1293.4	2916.1	5179.0	448.26	1293.9	2917.8	5185.3
10°	318.10	321.49	736.39	1293.5	317.77	321.60	736.59	1294.7
20°	78.552	167.74	321.48	331.25	78.580	167.91	321.85	331.15
30°	33.623	74.838	141.56	216.39	33.636	74.897	141.72	216.79
40°	17.963	41.425	78.631	122.18	17.969	41.455	78.720	122.40
	inextensible case							
	[Chidamparam and Leissa 1995]				Current approach			
α	mode 1	mode 2	mode 3	mode 4	mode 1	mode 2	mode 3	mode 4
5°	1293.5	2765.6	5181.5	7957.4	1293.9	2766.5	5186.9	7962.1
10°	321.51	690.04	1293.5	1987.9	321.60	690.43	1294.9	1991.1
20°	78.558	171.15	321.53	495.61	78.579	171.26	321.87	496.41
30°	33.626	75.080	141.58	219.26	33.635	75.125	141.73	219.61
40°	17.964	41.467	78.641	122.54	17.969	41.492	78.724	122.74

Table 2. Nondimensional free-vibration frequencies $\lambda = \omega R_r^2 \sqrt{m/EI}$ of pinned-pinned circular arches.

In Table 2, the dominant types of motion are identified for each mode. For $\alpha = 5°$ and 10° for the extensible case, the dominant motion in modes 1–4 are first symmetric bending, first antisymmetric bending, second symmetric bending, and second antisymmetric bending motions, respectively. For both the extensible case with $\alpha \geq 20°$ and the inextensible case, the dominant types of motion in modes 1–4 are first antisymmetric bending, second symmetric bending, second antisymmetric bending motions, and third symmetric bending, respectively. Only the extensible cases have unique frequencies of 448.26 and 317.77 for mode 1, which are identified as first symmetric bending modes.

The following discussion explains further about what contributes to the disappearance of the first symmetric bending for both extensible case with $\alpha \geq 20°$ and inextensible case. First, consider the free-vibration frequencies of $\alpha \geq 20°$ for both extensible and inextensible cases. Note that both frequencies are close to each other, especially as α increases. This is because of the low-frequency mode transition. By holding the beam's total length constant, a beam with a larger α has higher initial curvature. Because of this high initial curvature, the frequencies of certain modes change from one value to another while simultaneously the corresponding dominant type of motion for that mode is changing. (The next section has a more detailed explanation for this phenomenon.) Second, the first symmetric bending will be coupled strongly to the stretching mode. This explains why the mode is absent when the beam is inextensible.

The convergence of numerical solutions for a circular arch with $\alpha = 20°$ is tested as the number of elements increases. Figure 3 shows that the four lowest frequencies decrease monotonically as the number of elements increases. The relative difference between the results of $N = 80$ and 160 is less than 1%, and all the results presented here are for $N = 160$ elements.

	extensible case [Chidamparam and Leissa 1995]				Current approach			
α	mode 1	mode 2	mode 3	mode 4	mode 1	mode 2	mode 3	mode 4
5°	788.17	2021.7	3969.3	6226.8	788.34	2022.8	3972.3	6226.5
10°	388.56	503.49	999.44	1636.6	338.60	503.72	1000.3	1638.8
20°	123.96	209.32	338.91	406.99	124.02	209.45	339.03	407.54
30°	53.735	98.426	179.31	250.07	53.760	98.505	179.56	250.47
40°	29.215	55.020	99.680	145.38	29.228	55.066	99.818	145.67
	inextensible case [Chidamparam and Leissa 1995]				Current approach			
α	mode 1	mode 2	mode 3	mode 4	mode 1	mode 2	mode 3	mode 4
5°	2021.9	3641.9	6557.9	9500.9	2022.8	3635.4	6566.8	9466.0
10°	503.54	909.14	1637.2	2373.7	503.76	909.86	1639.4	2378.4
20°	123.97	225.96	407.11	592.01	124.03	226.14	407.65	593.16
30°	53.740	99.458	179.36	262.06	53.762	99.536	179.60	262.57
40°	29.217	55.194	99.705	146.58	29.230	55.238	99.837	146.87

Table 3. Nondimensional free-vibration frequencies $\lambda = \omega R_r^2\sqrt{m/EI}$ of clamped-clamped circular arches.

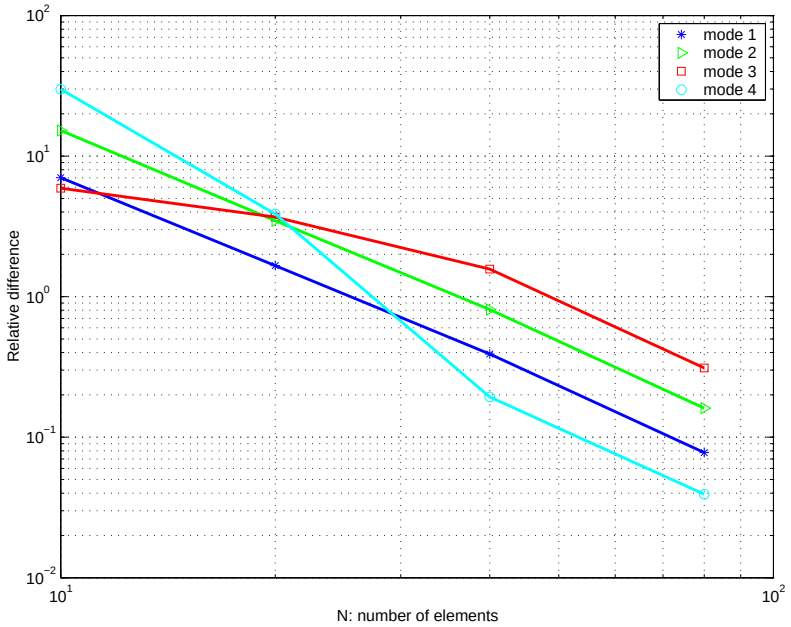

Figure 3. Relative differences of nondimensional free-vibration frequencies $\lambda = \omega R_r^2\sqrt{m/EI}$ for $N = 10, 20, 40$, and 80 with respect to $N = 160$ of pinned-pinned circular arches with $\alpha = 20°$.

	$\sigma_2 = \sigma_3 = 20$											
	[Irie et al. 1982]				[Howson and Jemah 1999]				present			
α	m1	m2	m3	m4	m1	m2	m3	m4	m1	m2	m3	m4
30°	16.74	36.92*	40.45	69.92	16.743	36.921*	40.449	69.618	16.579	36.398	40.232	68.711
60°	4.282	11.69	22.05*	22.38	4.2836	11.768	22.045*	22.379	4.2606	11.644	21.875*	22.329
90°	1.776	4.982	10.13	16.76	1.7764	4.9814	10.133	16.762	1.7687	4.9584	10.111	16.778

	$\sigma_2 = \sigma_3 = 100$											
	[Irie et al. 1982]				[Howson and Jemah 1999]				present			
α	m1	m2	m3	m4	m1	m2	m3	m4	m1	m2	m3	m4
30°	19.40	54.03	105.6	172.8	19.401	54.029	105.65	172.77	19.385	54.049	105.88	173.52
60°	4.451	12.83	25.99	43.57	4.4512	12.826	25.988	43.570	4.4444	12.810	25.990	43.630
90°	1.804	5.198	10.92	18.72	1.8042	5.1975	10.917	18.725	1.7998	5.1857	10.905	18.727

Table 4. Nondimensional free-vibration frequencies $\lambda = \omega R_r^2 \sqrt{m/(EI)_3}$ of clamped-clamped circular arches ($*$ represents modes in which torsion is dominant; m1 stands for mode 1, etc.)

Example: out-of-plane free-vibration of a curved beam with different half-angles. The out-of-plane free-vibration frequencies of a clamped-clamped arch with square cross-section are shown in Table 4 for two different slenderness ratios ($\sigma_2 = \sigma_3 = 20$ and 100). The slenderness ratio $\sigma_2^2 = A R_r^2 / I_2$ is expressed in terms of the cross-sectional area A, the radius of curvature R_r, and the second moment of area I_2; similar relations apply to σ_3. The beam length is 5 m. The out-of-plane free-vibration frequencies are shown in Table 4 with the ones from [Irie et al. 1982; Howson and Jemah 1999] and they are very close to each other. The material properties and cross-sectional constants for each case are listed in Table 1. It should be noted that these results include shear deformation and rotary inertia; particularly for smaller values of σ_2 and σ_3, results are more accurate when these phenomena are included in the calculations. The present results are based on section constants from VABS, values of which may differ slightly from the approximations used in [Irie et al. 1982; Howson and Jemah 1999].

6. Coupled free-vibration frequencies for initially curved beams

In this section the coupled free-vibration characteristics of beams with various values of initial curvature k_2 are examined. No external forces and moments are applied to beams. The free-vibration frequencies of beams with free-free, clamped-clamped, and pinned-pinned boundary conditions are shown in Figure 4 and Table 5 for various values of initial curvature k_2. The length of the beam is 10 m; the width and height are 0.1 m. The material properties are taken to be those of aluminum: $E = 7 \times 10^{10}\,\mathrm{N/m^2}$, $G = 2.55 \times 10^{10}\,\mathrm{N/m^2}$, and $\rho = 2700\,\mathrm{kg/m^3}$.

The eight lowest-frequency modes of beams with various levels of initial curvature are identified, and the frequencies are plotted in Figure 4 and given in Table 5. For the cases of low initial curvatures, modes 1, 2, 3, 4, ..., correspond to the modes for which the dominant motions are first symmetric out-of-plane

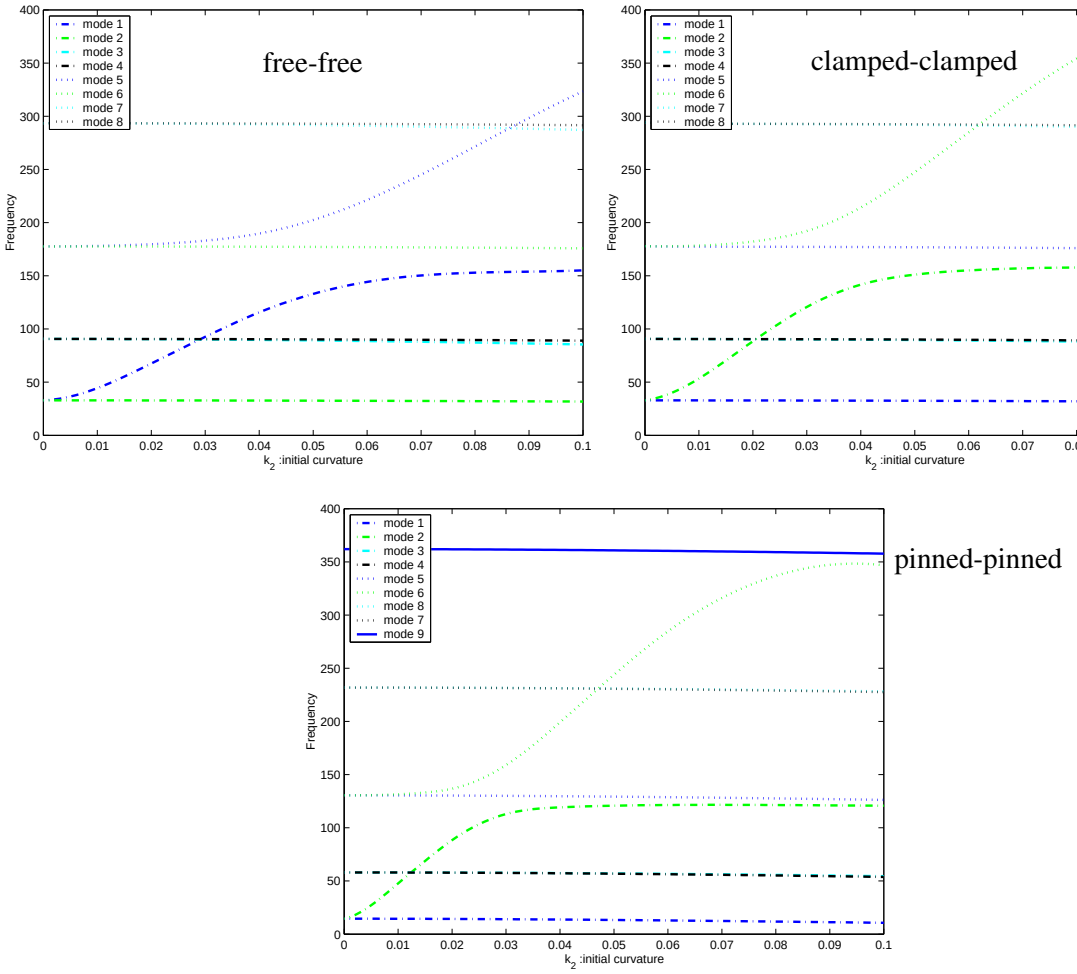

Figure 4. Vibration frequency versus initial curvature k_2 for initially curved beams with different boundary conditions.

bending (1OB), first symmetric in-plane bending (1IB), first antisymmetric out-of-plane bending (1AOB), first antisymmetric in-plane bending (1AIB), etc., respectively. The plots show that for the free-free case, the frequency of mode 1 departs from the one for zero initial curvature and approaches the one for mode 5. The dominant type of motion also changes from 1OB to 2OB as the initial curvature increases. The four lowest mode shapes for a beam with initial curvature $k_2 = 0.10$ are shown in Figure 5. The dominant motion of mode 1 transitions from 1OB to 2OB when the initial curvature becomes larger.

On the other hand, for both clamped-clamped and pinned-pinned boundaries, the frequency of mode 2 changes from the one for zero initial curvature and approaches to the one for mode 6. Its dominant motion changes from 1IB to 2IB. Figure 6 shows the mode transition of mode 2 from dominant 1IB to dominant 2IB as the initial curvature k_2 increases for the pinned-pinned case. This phenomenon, which is often referred to as veering [Chen and Ginsberg 1992] or frequency mode transition [Tarnopolskaya et al. 1996; Tarnopolskaya et al. 1999], results from the nature of the eigenvalues of a general self-adjoint

Free-free boundary condition								
k_2	mode 1	mode 2	mode 3	mode 4	mode 5	mode 6	mode 7	mode 8
0.00	32.885	32.885	90.629	90.629	177.61	177.61	293.45	293.45
0.02	67.530	32.836	90.407	90.564	179.66	177.54	293.18	293.38
0.04	115.64	32.694	89.746	90.368	189.71	177.32	292.37	293.15
0.06	144.23	32.462	88.668	90.042	221.34	176.96	291.06	292.78
0.08	152.93	32.151	87.208	89.591	271.52	176.47	289.29	292.26
0.10	155.13	31.772	85.408	89.018	323.39	175.83	287.11	291.58
Clamped-clamped boundary condition								
k_2	mode 1	mode 2	mode 3	mode 4	mode 5	mode 6	mode 7	mode 8
0.00	32.882	32.882	90.660	90.660	177.81	177.81	294.14	294.14
0.02	32.810	88.424	90.472	90.398	177.31	182.21	292.91	292.82
0.04	32.639	141.65	90.235	89.940	177.05	214.22	292.63	292.29
0.06	32.365	155.10	89.844	89.188	176.62	284.85	292.18	291.41
0.08	32.003	157.82	89.304	88.156	176.01	354.19	291.55	290.20
0.10	31.571	158.24	88.622	86.863	175.25	393.53	290.73	288.68
Pinned-pinned boundary condition								
k_2	mode 1	mode 2	mode 3	mode 4	mode 5	mode 6	mode 7	mode 8
0.00	14.506	14.506	58.011	58.011	130.48	130.48	231.85	231.85
0.02	14.307	57.811	57.865	88.397	130.28	136.74	231.65	231.70
0.04	13.739	57.234	57.428	119.21	129.70	199.11	231.07	231.26
0.06	12.880	56.331	56.712	121.43	128.79	230.16	230.53	284.68
0.08	11.825	55.167	55.732	121.40	127.62	228.99	229.54	336.91
0.10	10.665	53.794	54.509	120.75	126.21	227.58	228.28	346.84

Table 5. Vibration frequencies versus initial curvature k_2 for free-free, clamped-clamped, and pinned-pinned boundary conditions.

system when a certain parameter changes in the system. In the present study, it is the initial curvature k_2 that changes.

7. Coupled vibration of initially curved beams under end moments

Now the vibration characteristics of curved beams are considered, including beams both with curvature that is built-in and curvature that occurs because the beam is loaded with end moments. The section properties vary according to the initial curvature. Sample results are given in Table 6 on page 688. (Material properties are the same as those given in the previous section.) In the general case we consider an beam with various initial curvatures k_2, loaded under various equal and opposite values of applied moments at the ends giving rise to a constant value of bending moment $\overline{M}_2$. To facilitate this parametric study, the total static equilibrium value of curvature $\overline{K}_2$ is divided into two parts: the initial curvature k_2

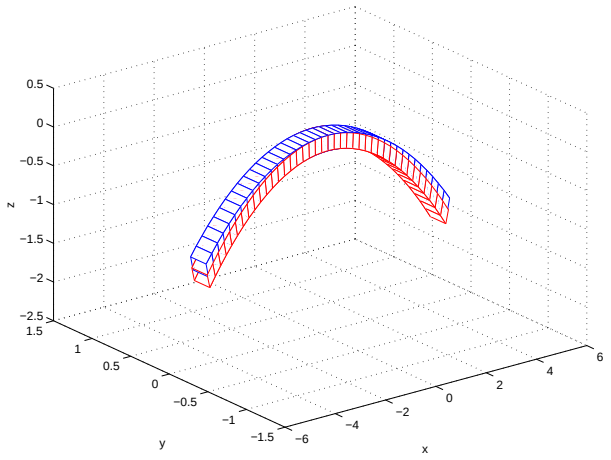

mode 2 (dominant 1IB: 31.772 rad/sec)

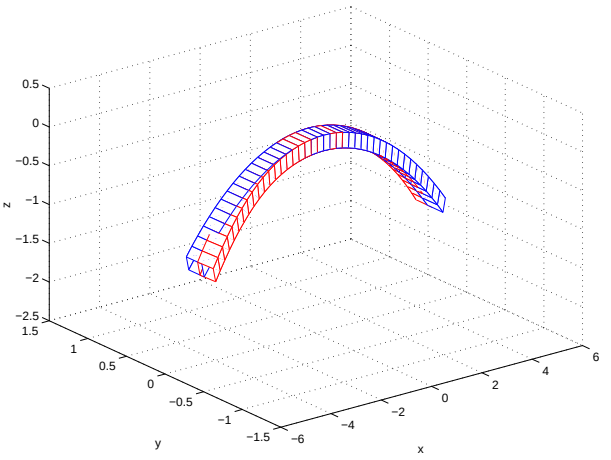

mode 3 (dominant 1AOB: 85.408 rad/sec)

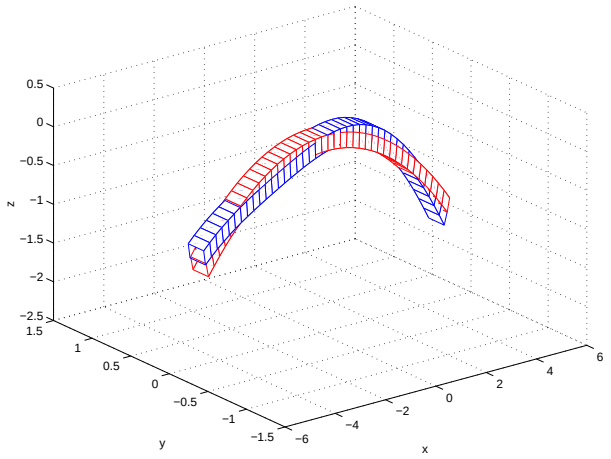

mode 4 (dominant 1AIB: 89.018 rad/sec)

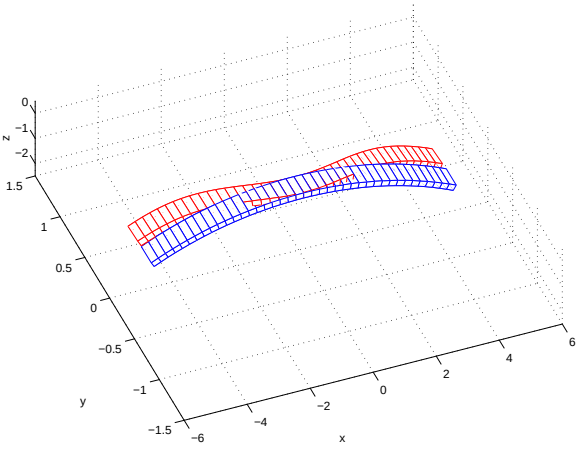

mode 1 (dominant 2OB: 155.13 rad/sec)

Figure 5. Four lowest modes of an initially curved free-free beam ($k_2 = 0.10$).

and the curvature caused by the applied end moments $\overline{M}_2/EI_2$. The total curvature is then

$$\overline{K}_2 = k_2 + \frac{\overline{M}_2}{EI_2} \tag{21}$$

where EI_2 is the vertical bending stiffness for bending in the plane of the initially curved beam. A nondimensional curvature ratio β is then introduced as the ratio of the initial curvature to the final total curvature and defined as

$$\beta = \frac{k_2}{\overline{K}_2} \qquad (\overline{K}_2 \neq 0) \tag{22}$$

For example, if $\beta = 0$, the beam has a zero initial curvature. If $\beta = 1$, the beam's initial curvature is the total curvature, which means that no end moments will be applied. If $\beta = -1$, the beam has an opposite initial curvature to the final configuration. Figure 7 shows initial configurations of beam with

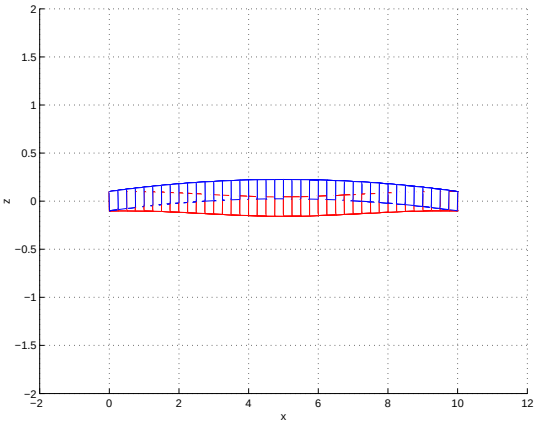

$k_2 = 0.01$

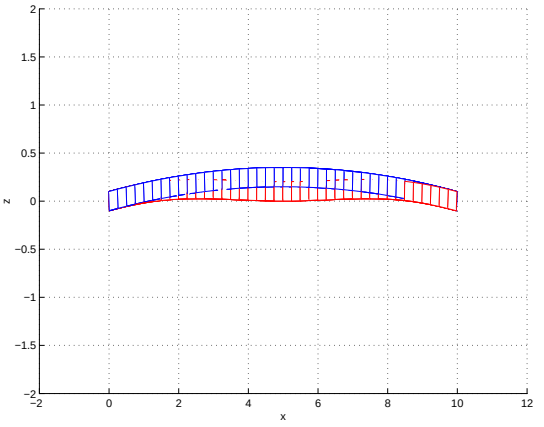

$k_2 = 0.02$

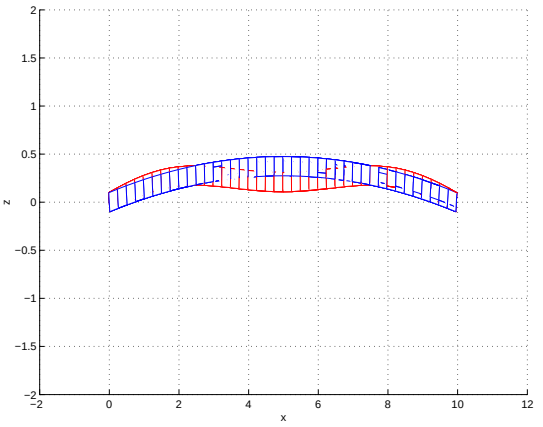

$k_2 = 0.03$

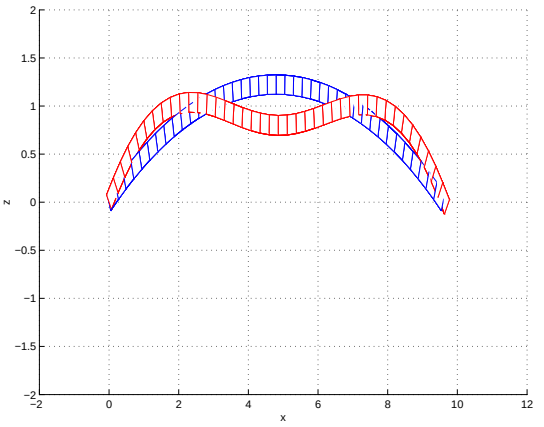

$k_2 = 0.10$

Figure 6. Mode transition of initially curved pinned-pinned beams (mode 2).

R_r	1/0.1	1/0.07	1/0.04	1/0.01
R_{11}	1.4286e-09	1.4286e-09	1.4286e-09	1.4286e-09
R_{22}	4.7292e-09	4.7291e-09	4.7291e-09	4.7291e-09
R_{33}	4.7291e-09	4.7291e-09	4.7291e-09	4.7291e-09
S_{12}	3.4133e-10	2.3790e-10	1.3619e-10	3.4476e-11
S_{21}	−1.1431e-12	8.6327e-13	9.5232e-14	−6.7113e-13
T_{11}	2.7802e-06	2.7803e-06	2.7803e-06	2.7803e-06
T_{22}	1.7143e-06	1.7143e-06	1.7143e-06	1.7143e-06
T_{33}	1.7143e-06	1.7143e-06	1.7143e-06	1.7143e-06
ξ_3	8.7588e-05	6.1310e-05	3.5034e-05	8.7585e-06

Table 6. Nonzero cross-sectional constants used for calculation of coupled free-vibration frequencies for initially curved beams (flexibility submatrices R_{ij}, S_{ij}, T_{ij}, radius of curvature R_r, and shear center location ξ_3).

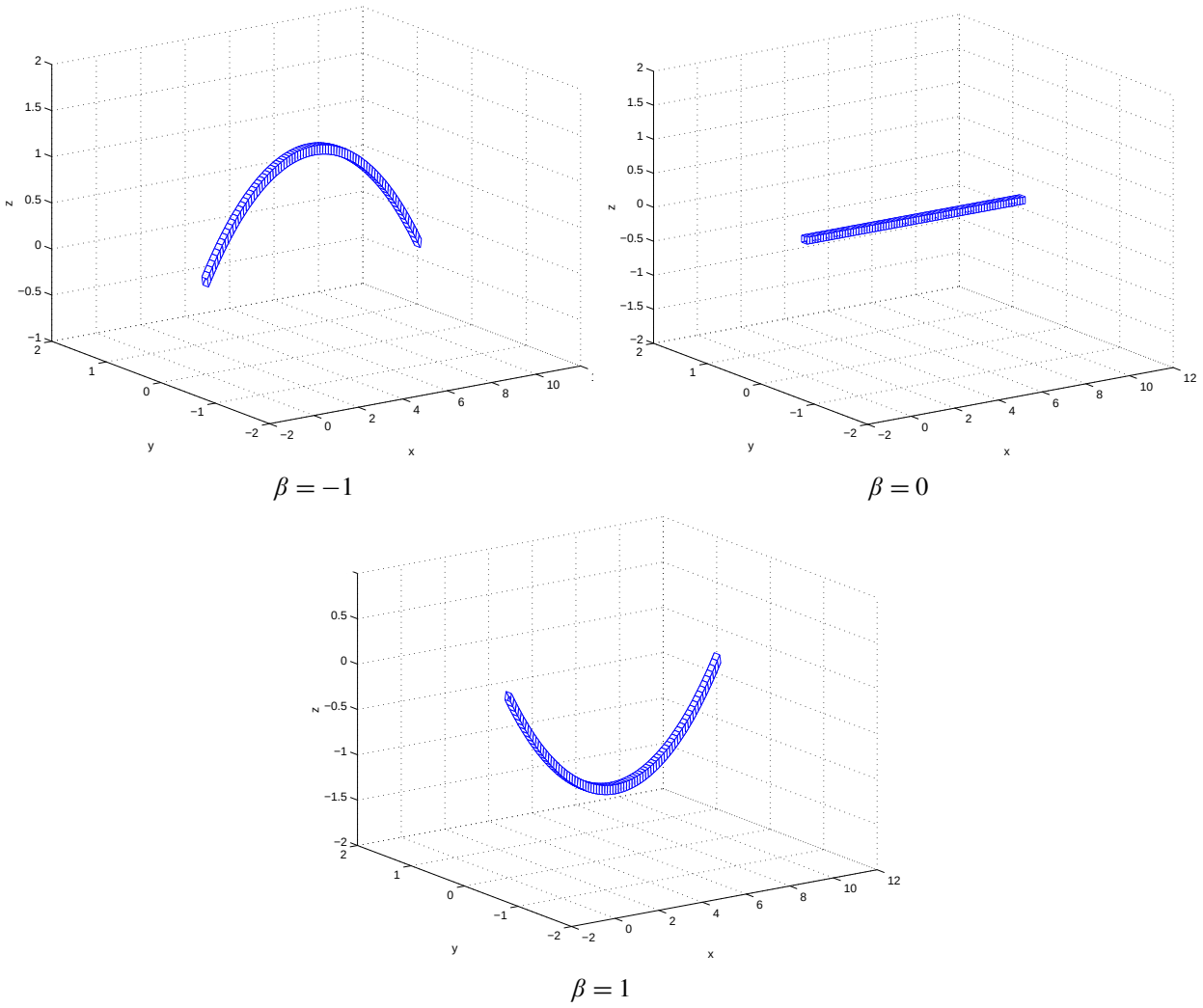

Figure 7. Initial configurations of beams with different β.

β	mode 1	mode 2	mode 3	mode 4	mode 5	mode 6
0	31.842	32.548	89.567	90.630	177.94	179.13
0.1	31.842	96.606	89.567	90.209	177.94	185.45
0.2	31.842	125.16	89.567	89.776	177.94	199.11
0.3	31.842	140.08	89.332	89.568	177.94	211.83
0.4	31.842	147.61	88.878	89.568	177.94	229.92
0.5	31.842	151.58	88.412	89.568	177.95	248.30

Table 7. Vibration frequencies versus curvature ratio β for initially curved free-free beams.

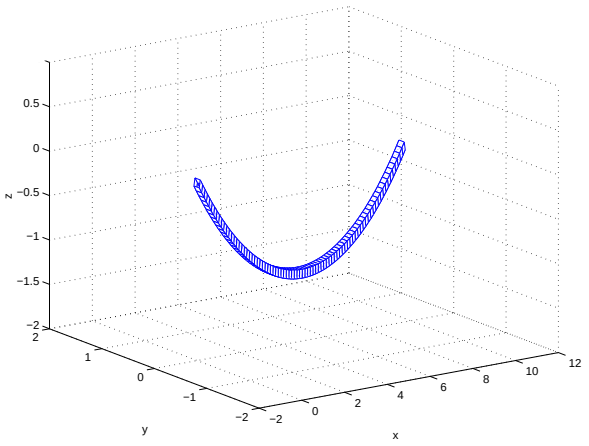

Figure 8. Final deformed configuration ($\overline{K}_2 = -0.10$) with end moments.

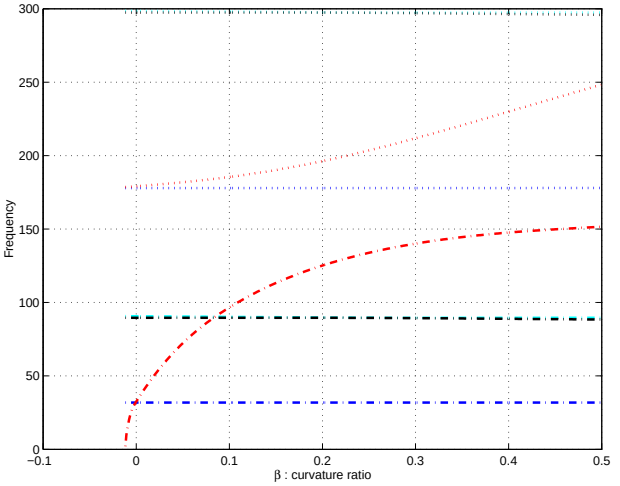

Figure 9. Vibration frequencies versus curvature ratio β for beams under end moments.

$\beta = -1, 0, 1$. (One can picture intermediate configurations of different β.) End moments are applied to deform the beam with various β so that $\overline{K}_2 = -0.10$ as shown in Figure 8. A rectangular cross-section is chosen to determine beam properties. The ratio r of height h to width b can be defined as

$$r = \frac{h}{b} \tag{23}$$

Table 7 on the previous page and Figure 9 show the vibration frequencies for various β. It is noticeable that frequencies for modes 2 and 6 change depending on β, which here indicates the value of initial curvature k_2. The frequency of mode 2, in which the dominant motion is the first out-of-plane bending motion, decreases as β decreases, becoming zero when $\beta = -0.0117$, indicating a lateral-torsional

buckling instability. As the initial curvature approaches close to that of the opposite sign of the final total curvature $\bar{K} = -0.10$ (i.e. β becomes a larger negative value), the larger end moments apply. For β lower than the critical value β_{cr}, the eigenvalues for mode 2 become pure real, which indicates that the mode is unstable.

8. Conclusion

The paper describes numerical procedures used to investigate the coupled free-vibration of curved beams, both initially curved and curved because of loading. Present results agree well with those from published papers. The governing equations of the present approach do not require displacement and rotation variables. Even in cases where displacement and rotation variables appear in the boundary conditions, this does not prohibit the use of the formulation. The reason is that these variables can be easily recovered from the formulation (i.e. they are secondary variables and can be expressed in terms of the primary variables). This feature makes the whole analysis quite concise.

The analysis provides the spectrum of free-vibration frequencies for given arbitrary configurations. The corresponding vibration mode shapes are easily visualized in order to observe which types of motion are dominant and which others are associated with the mode. The numerical examples show that it is necessary to include extensibility for beams with small initial curvature. Otherwise, one cannot observe those modes that are coupled to stretching motion. Note that low-frequency mode transition exists for beams with high initial curvatures.

The coupled free-vibration shows that the behaviors of simple engineering beam free-vibration problems are significantly different when beams are initially curved. The variation depends on the values of initial curvature and the types of boundary conditions. For certain regions of initial curvatures, the frequency and dominant motion of certain modes transition from the ones for zero initial curvature to those for the next higher mode. The shear center and neutral axis locations, as is true for the cross-sectional elastic constants, change as functions of initial curvature.

The case of end-loaded beams is also considered. In particular, when the geometries of an initially curved beam and an end-loaded beam are the same, results obtained demonstrate significant differences in behavior. Loading an initially curved beam affects the vibration characteristics and may lead to lateral-torsional buckling instability. Additional work should be done to address the instabilities of such configurations.

References

[Cesnik and Hodges 1997] C. E. S. Cesnik and D. H. Hodges, "VABS: a new concept for composite rotor blade cross-sectional modeling", *J. Am. Helicopter Soc.* **42**:1 (1997), 27–38.

[Chen and Ginsberg 1992] P.-T. Chen and J. H. Ginsberg, "On the relationship between veering of eigenvalue loci and parameter sensitivity of eigenfunctions", *J. Vib. Acoust.* (*ASME*) **114**:2 (1992), 141–148.

[Chidamparam and Leissa 1993] P. Chidamparam and A. W. Leissa, "Vibrations of planar curved beams, rings and arches", *Appl. Mech. Rev.* **46**:9 (1993), 467–483.

[Chidamparam and Leissa 1995] P. Chidamparam and A. W. Leissa, "Influence of centerline extensibility on the in-plane free vibrations of loaded circular arches", *J. Sound Vib.* **183**:5 (1995), 779–795.

[Fung 2004] T. C. Fung, "Improved approximate formulas for the natural frequencies of simply supported Bernoulli–Euler beams with rotational restrains at the ends", *J. Sound Vib.* **273**:1–2 (2004), 451–455.

[Hodges 1999] D. H. Hodges, "Non-linear inplane deformation and buckling of rings and high arches", *Int. J. Non-Linear Mech.* **34**:4 (1999), 723–737.

[Hodges 2003] D. H. Hodges, "Geometrically exact, intrinsic theory for dynamics of curved and twisted anisotropic beams", *AIAA J.* **41**:6 (2003), 1131–1137.

[Hodges 2006] D. H. Hodges, *Nonlinear composite beam theory*, Progress in Astronautics and Aeronautics **213**, AIAA, Reston, VA, 2006.

[Howson and Jemah 1999] W. Howson and A. Jemah, "Exact out-of-plane natural frequencies of curved Timoshenko beams", *J. Eng. Mech.* (*ASCE*) **125**:1 (1999), 19–25.

[Irie et al. 1982] T. Irie, G. Yamada, and K. Tanaka, "Natural frequencies of out-of-plane vibration of arcs", *J. Appl. Mech.* (*ASME*) **49** (1982), 910–913.

[Patil and Hodges 2006] M. J. Patil and D. H. Hodges, "Flight dynamics of highly flexible flying wings", *J. Aircr.* **43**:6 (2006), 1790–1799.

[Tarnopolskaya et al. 1996] T. Tarnopolskaya, F. de Hoog, N. H. Fletcher, and S. Thwaites, "Asymptotic analysis of the free in-plane vibrations of beams with arbitrarily varying curvature and cross-section", *J. Sound Vib.* **196**:5 (1996), 659–680.

[Tarnopolskaya et al. 1999] T. Tarnopolskaya, F. R. de Hoog, and N. H. Fletcher, "Low-frequency mode transition in the free in-plane vibration of curved beams", *J. Sound Vib.* **228**:1 (1999), 69–90.

[Yu et al. 2002] W. Yu, V. V. Volovoi, D. H. Hodges, and X. Hong, "Validation of the variational asymptotic beam sectional analysis", *AIAA J.* **40**:10 (2002), 2105–2112.

Received 4 Mar 2008. Revised 24 Sep 2008. Accepted 25 Sep 2008.

CHONG-SEOK CHANG: juliera324@hotmail.com
Georgia Institute of Technology, School of Aerospace Engineering, 270 Ferst Drive, Atlanta, GA 30332-1510, United States

DEWEY H. HODGES: dhodges@gatech.edu
Georgia Institute of Technology, School of Aerospace Engineering, 270 Ferst Drive, Atlanta, GA 30332-1510, United States
http://www.ae.gatech.edu/~dhodges/